Crystal Structure and Optical Spectroscopy of $Er_2[Pt(CN)_4]_3 \cdot 21H_2O$ and $Er_2[Pt(CN)_4]_2 \cdot SO_4 \cdot 11.5H_2O$

Andreas Loosli, Markus Wermuth, and Hans-Ueli Güdel*

Departement für Chemie und Biochemie, Universität Bern, Freiestrasse 3, 3000 Bern 9, Switzerland

Silvia Capelli, Jürg Hauser, and Hans-Beat Bürgi

Laboratorium für Chemische und Mineralogische Kristallographie, Universität Bern, Freiestrasse 3, 3000 Bern 9, Switzerland

Received September 23, 1999

We have synthesized two forms of erbium tetracyanoplatinates, $Er_2[Pt(CN)_4]_3 \cdot 21H_2O$ (red form) and $Er_2[Pt(CN)_4]_2 \cdot SO_4 \cdot 11.5H_2O$ (yellow form), and determined their crystal structures by X-ray diffraction. While the red form crystallizes in the orthorhombic space group *Pbcn*, with $a = 15.4848(3)$ Å, $b = 13.8186(2)$ Å, $c = 19.07820(10)$ Å, $\alpha = \beta = \gamma = 90°$, and $Z = 4$, the yellow form precipitates in the tetragonal space group *I*4*cm*, with $a = b = 14.321(2)$ Å, $c = 13.338(3)$ Å, $\alpha = \beta = \gamma = 90°$, and $Z = 4$. Both forms show $[Pt(CN)_4]^{2-}$ chains but differ markedly in color and morphology. This is due to the incorporation of sulfate ions in the latter modification, leading to an increased Pt−Pt distance. The observed optical absorption and emission behavior of the title compounds is correlated with the Pt−Pt distances.

1. Introduction

The compounds $Ln_2[Pt(CN)_4]_3 \cdot nH_2O$ ($Ln^{3+} = La^{3+}...Er^{3+}$, Tm^{3+}, Yb^{3+}) belong to the big class of tetracyanoplatinates (CP) displaying $[Pt(CN)_4]^{2-}$ chains.[1−3] Unlike the alkali and alkaline earth tetracyanoplatinates, the $Ln_2[Pt(CN)_4]_3 \cdot nH_2O$ have been reported to exist in two forms: a yellow form (for $La^{3+}...Gd^{3+}$) and a red form (for $Tb^{3+}...Yb^{3+}$).[4] In the literature the existence of a yellow modification has also been mentioned for $Tb^{3+}...Yb^{3+}$ except for Er^{3+}.[1−3] The water content for the red and yellow forms of DyCP has been given as $21H_2O$ and $13.5H_2O$, respectively.[1−3] An orthorhombic unit cell with $a = 13.782(5)$ Å, $b = 15.463(4)$ Å, and $c = 19.044(6)$ Å was reported for the red form of ErCP, while for the yellow form no structural information exists.[1,2,5]

We were intrigued by these reports because it is well-known that the position of the first intense absorption band in the visible correlates with the Pt−Pt distance in the CP chains in a well-defined way.[6−8] It shows a red shift with decreasing Pt−Pt distance. On reducing the number of water molecules available per three $[Pt(CN)_4]^{2-}$ units from $n = 21$ to $n = 13.5$, one could reasonably expect a shortening of the Pt−Pt distance. But this is in contrast to the observed blue shift in the spectrum (color shift from red to yellow). We therefore decided to synthesize the red and yellow modification of ErCP and study their structural and spectroscopic properties. As it turned out and will be shown in detail below, sulfate ions are found in the structure of the yellow form, thus changing its stoichiometry to $Er_2[Pt(CN)_4]_2 \cdot SO_4 \cdot 11.5H_2O$ with straightforward consequences on the Pt−Pt distances and the color. To our knowledge, this difference in composition has not been noticed before.

The absorption and luminescence properties of the CP family have been studied in detail by Gliemann and Yersin.[1,2] Similar to the absorption edge, the position of the luminescence band was found to be correlated with the Pt−Pt distance. In a beautiful set of experiments this distance was tuned by chemical variation,[9,10] temperature,[11] pressure,[12−15] and an external magnetic field.[16,17] In LnCP (Ln = Sm, Eu) it was found that the Pt exitation could be transferred nonradiatively to Sm^{3+} or Eu^{3+}, leading to Sm^{3+} and Eu^{3+} luminescence, respectively.[4,18−20]

In the following, we present the selective synthesis of the two forms of LnCP, exemplified by the Er^{3+} salts, their crystal structures, and optical spectra in the visible and near-IR. We

* To whom correspondence should be addressed.

(1) Gliemann, G.; Yersin, H. *Struct. Bonding* **1985**, *62*, 87.
(2) Yersin, H. *Habilitationsschrift*; Universität Regensburg, 1979.
(3) Holzapfel, W.; Yersin, H.; Gliemann, G. *Z. Kristallogr.* **1981**, *157*, 47.
(4) von Ammon, W.; Gliemann, G. *J. Chem. Phys.* **1982**, *77*, 2266.
(5) Daniels, W.; Yersin, H.; von Philipsborn, H.; Gliemann, G. *Solid State Commun.* **1979**, *30*, 353.
(6) Day, P. *J. Am. Chem. Soc.* **1975**, *97*, 1588.
(7) Yersin, H.; Gliemann, G. *Ber. Bunsen-Ges. Phys. Chem.* **1975**, *79*, 1050.
(8) Yersin, H.; Gliemann, G.; Rössler, U. *Solid State Commun.* **1977**, *21*, 915.
(9) Holzapfel, W.; Yersin, H.; Gliemann, G. *J. Chem. Phys.* **1981**, *74* (4), 2124.
(10) Holzapfel, W.; Gliemann, G. *Ber. Bunsen-Ges. Phys. Chem.* **1985**, *89*, 935.
(11) Holzapfel, W.; Yersin, H.; Gliemann, G.; Otto, H. H. *Ber. Bunsen-Ges. Phys. Chem.* **1978**, *82*, 207.
(12) Stock, M.; Yersin, H. *Chem. Phys. Lett.* **1976**, *40*, 423.
(13) Stock, M.; Yersin, H. *Solid State Commun.* **1978**, *27*, 1305.
(14) Yersin, H.; Hidvegi, I.; Gliemann, G.; Stock, M. *Phys. Rev. B* **1979**, *19*, 177.
(15) Lechner, A.; Gliemann, G. *J. Am. Chem. Soc.* **1989**, *111*, 7469.
(16) Hidvegi, I.; von Ammon, W.; Gliemann, G. *J. Am. Chem.* **1982**, *76*, 4361.
(17) von Ammon, W.; Hidvegi, I.; Gliemann, G. *J. Am. Chem.* **1984**, *80* (6), 2837.
(18) Yersin, H.; Stock, M. *J. Chem. Phys.* **1982**, *76* (5), 2136.
(19) Yersin, H.; von Ammon, W.; Stock, M.; Gliemann, G. *J. Lumin.* **1979**, *18/19*, 774.
(20) Yersin, H *J. Chem. Phys.* **1978**, *68* (10), 4707.

10.1021/ic991137x CCC: $19.00
Published on Web 05/02/2000

finally correlate the positions of the Pt absorptions with the Pt−Pt distances in the red and yellow compounds.

2. Experimental Section

Synthesis and Characterization. Both forms, $Er_2[Pt(CN)_4]_3 \cdot 21H_2O$ as well as $Er_2[Pt(CN)_4]_2 \cdot SO_4 \cdot 11.5H_2O$, were obtained by similar two-step syntheses. In the first step erbium sulfate was prepared by dissolving erbium oxide (Alfa, 99.999% purum) in a sulfuric acid solution (Merck, 95−97%) according or analogous to literature preparations.[21,22] The final product was subsequently obtained by dissolving erbium sulfate and $Ba[Pt(CN)_4] \cdot 4H_2O$ (BaCP) (Heraeus; Pt, 38.31%) in sulfuric acid by heating. The precipitated barium sulfate was filtered off, and well-shaped crystals of the title compounds were grown from acidic aqueous solution by slow evaporation of the solvent. $Er_2[Pt(CN)_4]_3 \cdot 21H_2O$ was obtained from a 0.3 M sulfuric acid solution, whereas the formation of $Er_2[Pt(CN)_4]_2 \cdot SO_4 \cdot 11.5H_2O$ could be induced by crystallizing from a sulfuric acid concentration of at least 1 M. While the former crystals were obtained as cherry-red thin plates, the latter ones grew as yellow, very thin needles. Both the red and the yellow crystals could only be cleaved perpendicular to the $[Pt(CN)_4]^{2-}$ chains.

Crystal Structure Determination. For the crystal structure determinations of $Er_2[Pt(CN)_4]_3 \cdot 21H_2O$ (red form) and $Er_2[Pt(CN)_4]_2 \cdot SO_4 \cdot 11.5H_2O$ (yellow form), single crystals of dimensions $0.1 \times 0.08 \times 0.06$ mm^3 and $0.3 \times 0.08 \times 0.05$ mm^3, respectively, were used. X-ray diffraction data were collected at room temperature on a Siemens Smart-CCD diffractometer using graphite-monochromated Mo Kα radiation ($\lambda = 0.710\ 73$ Å).

A total of 1271 frames (yellow form: 2182) with a step width of 0.3° in ω and an exposure time of 10 s were collected, corresponding to a hemisphere (yellow form: full sphere) of intensity data. Cell constants were obtained by least-squares refinement on the 2θ values of 4516 (yellow form: 1660) independent reflections in the range $1.98° < 2\theta < 27.51°$ (yellow form: $2.84° < 2\theta < 27.84°$). The collected frames were processed with the SAINT program,[23] which also performs Lorentz and polarization corrections. The intensities of weak reflections were corrected for $\lambda/2$ effects.[24] An empirical absorption correction on the basis of equivalent reflection intensities was applied with the program SADABS.[25,26]

The structures were solved by direct methods and difference Fourier analysis using the program SHELXS97.[27] The refinements were done by full-matrix least-squares procedures on F^2 using SHELXL97.[28] The hydrogen atoms could not be located. In the red form all atoms were refined anisotropically. In the yellow form all but the sulfate O atoms were refined anisotropically. The crystal data are collected in Table 1. The unit cell constants of the red form could be compared with those reported in the literature.[5]

Optical Spectroscopy. Absorption spectra of single crystals were measured on a Cary 5E UV−VIS−NIR spectrometer with fixed spectral bandwidths of 0.4 nm (UV/VIS) and 0.6 nm (NIR). The light polarization was parallel or perpendicular to the Pt chains (*c* axis). The crystal was cooled in a displex closed cycle helium cryostat HC-Z (APD Cryogenics Inc.).

For luminescence experiments the crystals were cooled in a double-wall helium gas flow tube. The excitation source was an argon ion laser (model 5490ASL-OOC, Ion Laser Technology) with the 457.9 nm line. The luminescence was passed through a double monochromator (Spex 1402, Spex Industries Inc.) and detected by a red-sensitive photomultiplier (Hamamatsu E2762-01). Instrument control and data collection were performed with a PC.

All absorption and emission spectra were analyzed using IGOR (WaveMetrics Inc.).

Table 1. Crystallographic Data for $Er_2[Pt(CN)_4]_3 \cdot 21H_2O$ (Red Form) and $Er_2[Pt(CN)_4]_2 \cdot SO_4 \cdot 11.5H_2O$ (Yellow Form)

	red form	yellow form
empirical formula	$C_{12}H_{42}N_{12}O_{21}Pt_3Er_2$	$C_8H_{23}N_8O_{15.5}SPt_2Er_2$
M_r (g mol^{-1})	1610.37	1236.05
temp (K)	293(2)	293(2)
λ (Mo Kα) (Å)	0.710 73	0.710 73
space group	*Pbcn* (No. 60)	*I4cm* (No. 108)
a (Å)	15.4848(3)	14.321(2)
b (Å)	13.8186(2)	14.321(2)
c (Å)	19.07820(10)	13.338(3)
α (deg)	90	90
β (deg)	90	90
γ (deg)	90	90
vol [Å^3]	4082.32(10)	2735.5(8)
Z	4	4
ρ_{calc} (g cm^{-3})	2.620	3.001
μ (mm^{-1})	14.392	16.421
R1[a] [$I > 2\sigma(I)$]	0.0274	0.0255
wR2[b] (all data)	0.0677	0.0555

[a] $R1 = \sum(|F_o| - |F_c|)/\sum|F_o|$. [b] $wR2 = [\sum w(F_o^2 - F_c^2)/\sum wF_o^2]^{1/2}$; $w = 1/[\sigma^2(F_o^2) + (aP)^2 + bP]$; $P = (F_o^2 + 2F_c^2)/3$.

Results and Discussion

Crystal Structure. The crystal structures of red $Er_2[Pt(CN)_4]_3 \cdot 21H_2O$ and of yellow $Er_2[Pt(CN)_4]_2 \cdot SO_4 \cdot 11.5H_2O$, although similar, show distinct differences because of the different stoichiometries. These are illustrated in Figures 1 and 2.

The red form crystallizes in the orthorhombic space group *Pbcn*, while the yellow form belongs to the tetragonal space group *I4cm*. The two structures show a similar packing of chains of nearly square planar $[Pt(CN)_4]^{2-}$ units running parallel to the *c* axis. In the red form the $[Pt(CN)_4]^{2-}$ units are in staggered conformation (C−Pt−Pt−C torsion angles from 37.1(3)° to 40.1(3)°), and in the yellow form they are in alternating eclipsed and staggered conformation (C−Pt−Pt−C torsion angles 4.1-(3)° and 40.9(3)°). In neither of the two structures the Pt atoms within the chains are equidistant; respective distances are 3.1625(5) and 3.1891(3) Å in the red form (mean distance $R =$ 3.1758(8) Å), and 3.2687(9) and 3.4003(9) Å in the yellow form (mean distance $R = 3.3345(18)$ Å).

As may also be seen in Figure 1 Er atoms bridge two neighboring Pt chains by being coordinated to two cyanide groups one from each chain. In the yellow form sulfate anions located at $^1/_2$, 0, *z* together with H_2O molecules bridge adjacent Er complexes. In the red form H_2O molecules alone take on this role.

The differences between Pt distances become more intelligible by describing the structures in terms of layers stacked along the *c* axis. In the red form a mixed Pt,Er layer is followed by two Pt layers, separated by free waters of crystallization, and finally a mixed Pt,Er layer. The yellow form may be derived qualitatively from that of the red form by removing every third $[Pt(CN)_4]^{2-}$ layer from the red form and compensating charge by adding SO_4^{2-} ions to the Pt,Er layers. This leads to an alternating sequence of Pt,Er and Pt layers with alternating staggered and eclipsed $[Pt(CN)_4]^{2-}$ conformations as observed. The insertion of SO_4^{2-} ions leads to a polar crystal structure with *c* as the polar axis. The longest Pt−Pt distance (3.4003(9) Å) is observed in the yellow form between the eclipsed Pt,Er and Pt layers separated by sulfate anions. The two medium Pt−

(21) Tolstoi, N. A.; Trofimov, A. K.; Tkachuk, A. M.; Tkachuk, N. N. *Bull. Acad. Sci. USSR, Phys. Ser.* **1956**, *20*, 529.
(22) de Rassenfosse, A.; Brasseur, H. *Bull. Soc. R. Sci. Liege* **1935**, *4*, 277.
(23) *SMART-CCD Software*, version 4.05; Siemens Analytical X-ray Instruments Inc.: Madison, WI, 1996.
(24) Kirschbaum, K.; Martin, A.; Pinkerton, A. A. *J. Appl. Crystallogr.* **1997**, *30*, 514.
(25) Sheldrick, G. M. *SADABS: Program for Empirical Absorption Correction of Area Detector Data*; University of Göttingen: Göttingen, Germany, 1996.
(26) Blessing, R. H. *Acta Crystallogr.* **1995**, *A51*, 33.
(27) Sheldrick, G. M. *Acta Crystallogr.* **1990**, *A46*, 467.
(28) Sheldrick, G. M. *SHELXL97. Program for the Refinement of Crystal Structures*; University of Göttingen: Göttingen, Germany, 1997.

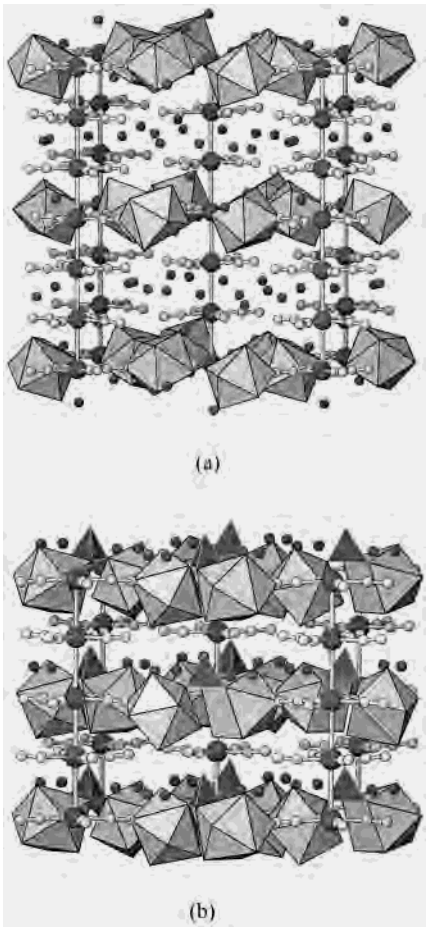

Figure 1. (a) Crystal packing of red $Er_2[Pt(CN)_4]_3 \cdot 21H_2O$: $Pt(CN)_4^{2-}$ chains running from bottom to top (*c* axis). The *a* axis is across the page. Every third $Pt(CN)_4^{2-}$ group is coordinated to four Er ions. The Er coordination spheres are represented as polyhedra. Nonbonded atoms represent free waters of crystallization. (b) Crystal packing of yellow $Er_2[Pt(CN)_4]_2 \cdot SO_4 \cdot 11.5H_2O$: $Pt(CN)_4^{2-}$ chains running from bottom to top (*c* axis). The *a* axis is across the page. Every second $Pt(CN)_4^{2-}$ group is coordinated to four Er ions. The Er coordination spheres and the sulfate anions are represented as polyhedra. Nonbonded atoms represent free waters of crystallization. Only one out of five disorder configurations is shown.

Pt distances (3.1891(3) and 3.2687(9) Å) are observed between staggered Pt and Pt,Er layers. The shortest Pt−Pt distance (3.1625(5) Å) is found in the red form between two staggered Pt layers separated only by water of crystallization.

The most important bond distances and angles for the two forms are listed in Tables 2 and 3, respectively; all others including positional parameters and displacement parameters are given in the Supporting Information.

In the red form there are two crystallographically inequivalent Pt atoms. The C−Pt−C and N−C−Pt angles are within 2.1° from 90° (from 87.9(3) to 91.8(3)°) and within 3.8° from 180° (from 176.2(7) to 177.5(6)°). The Pt−C and C−N distances vary from 1.981(6) to 2.013(7) Å and from 1.124(10) to 1.148(10) Å, respectively. The Er atom is coordinated to six H_2O molecules and to two cyanide N atoms from two different Pt chains. The Er−N distances are 2.393(6) and 2.392(6) Å, and the Er−O distances vary from 2.292(5) to 2.417(5) Å. The geometry of the Er sphere can be described as a distorted dodecahedron consisting of an elongated (O(1), O(6), N(1), N(2)) and a compressed tetrahedron (O(2), O(3), O(4), O(5)) that penetrate each other.

In the yellow form the Pt atoms have site symmetry 4. The

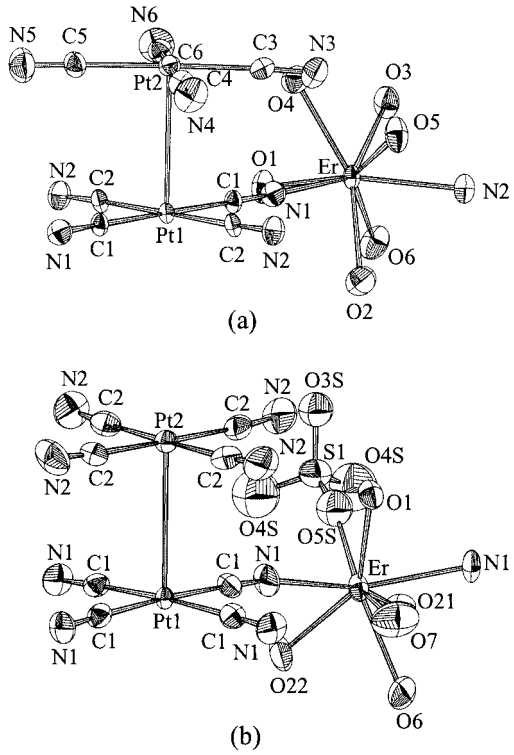

Figure 2. Molecular views and atom labeling schemes of $Er_2[Pt(CN)_4]_3 \cdot 21H_2O$ (a) and $Er_2[Pt(CN)_4]_2 \cdot SO_4 \cdot 11.5H_2O$ (b). In (b) only one of five disorder configurations is shown. All atoms are represented by 50% probability ellipsoids.

Table 2. Selected Bond Lengths (Å) and Angles (deg) for $Er_2[Pt(CN)_4]_3 \cdot 21H_2O$ (Red Form)[a]

Pt(1)−Pt(2)	3.1891(3)	Pt(2)−Pt(2)^{i}	3.1625(5)
Er−O(1)	2.292(5)	Er−O(5)	2.409(5)
Er−O(2)	2.339(5)	Er−O(6)	2.414(5)
Er−O(3)	2.334(5)	Er−N(1)	2.393(6)
Er−O(4)	2.417(5)	Er−N(2)^{ii}	2.392(6)
Pt(1)−C(1)	1.990(6)	Pt(1)−C(2)	1.981(6)
C(1)−N(1)	1.145(8)	C(2)−N(2)	1.143(8)
Pt(2)−C(3)	1.990(7)	Pt(2)−C(4)	2.000(7)
Pt(2)−C(5)	2.013(7)	Pt(2)−C(6)	1.993(7)
C(3)−N(3)	1.134(10)	C(4)−N(4)	1.148(10)
C(5)−N(5)	1.124(10)	C(6)−N(6)	1.144(10)
O(1)−Er−O(6)	70.8(2)	O(2)−Er−O(3)	146.5(2)
O(1)−Er−N(1)	78.8(2)	O(2)−Er−O(4)	143.11(19)
O(1)−Er−N(2)^{ii}	143.56(19)	O(2)−Er−O(5)	92.3(2)
O(6)−Er−N(1)	127.6(2)	O(3)−Er−O(4)	70.42(19)
O(6)−Er−N(2)^{ii}	74.4(2)	O(5)−Er−O(6)	143.14(19)
C(1)−Pt(1)−C(2)	91.0(3)		
C(3)−Pt(2)−C(4)	90.3(3)	C(3)−Pt(2)−C(5)	177.3(3)
C(3)−Pt(2)−C(6)	87.9(3)	C(4)−Pt(2)−C(5)	91.8(3)
C(4)−Pt(2)−C(6)	177.4(3)	C(5)−Pt(2)−C(6)	89.8(3)

[a] Symmetry code: (i) $-x, y, -z - 1/2$; (ii) $1/2 - x, -1/2 - y, -z$.

C−Pt−C and N−C−Pt angles are within 4.0(9)° from 90° and 180°, respectively. The Pt−C distances are 2.001(8) and 1.990(9) Å, and the C−N distances are 1.137(11) and 1.147(13) Å.

The Er coordination sphere and the sulfate anion in the yellow form are highly disordered. The disorder may be described as an overlay of five configurations. A detailed description is given in the Supporting Information.

Optical Spectroscopy. The luminescence, absorption, and reflection spectra of the red form of LnCP, including the red form of ErCP, have already been studied by Gliemann and Yersin.[1,2] The yellow form of ErCP has not yet been described

Table 3. Selected Bond Lengths (Å) and Angles (deg) for $Er_2[Pt(CN)_4]_2 \cdot SO_4 \cdot 11.5H_2O$ (Yellow Form)

Pt(1)−Pt(2)	3.2687(9)	Pt(1)−Pt(2)[i]	3.4003(9)
Er−O(1)	2.317(9)	Er−N(1)	2.430(7)
Er−O(21)	2.357(18)	Er−O(9)	2.16(4)
Er−O(22)	2.389(14)	Er−O(1S)	2.28(25)
Er−O(6)	2.42(2)	Er−O(4S)	2.81(3)
Er−O(7)	2.434(15)	Er−O(5S)[ii]	2.12(2)
Pt(1)−C(1)	2.001(8)	C(1)−N(1)	1.137(11)
Pt(2)−C(2)	1.990(9)	C(2)−N(2)	1.147(13)
C(1)−Pt(1)−C(1)[iii]	89.956(15)	C(2)−Pt(2)−C(2)[v]	89.995(6)
C(1)−Pt(1)−C(1)[iv]	176.8(5)	C(2)−Pt(2)−C(2)[iii]	179.1(5)

[a] Symmetry codes: (i) $x, -y, z + 1/2$; (ii) $1 - x, -y, z$; (iii) $-x, -y, z$; (iv) $y, -x, z$; (v) $-y, x, z$.

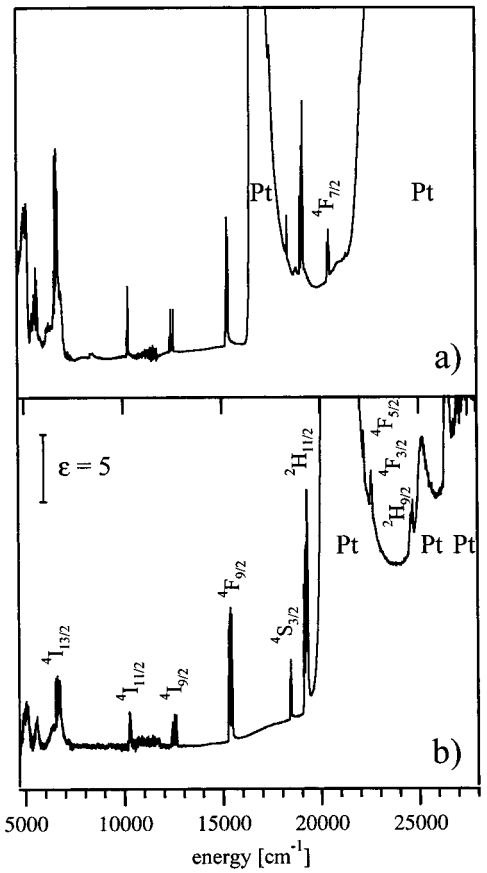

Figure 3. $\vec{E} \perp \vec{c}$ polarized absorption spectra of $Er_2[Pt(CN)_4]_3 \cdot 21H_2O$ (red form) (a) and $Er_2[Pt(CN)_4]_2 \cdot SO_4 \cdot 11.5H_2O$ (yellow form) (b) at 13 K.

in the literature. Figure 3 shows the $\vec{E} \perp \vec{c}$ polarized absorption spectra of $Er_2[Pt(CN)_4]_3 \cdot 21H_2O$ and $Er_2[Pt(CN)_4]_2 \cdot SO_4 \cdot 11.5H_2O$ at 13 K. The spectrum of $Er_2[Pt(CN)_4]_3 \cdot 21H_2O$ shows broad and intense transitions above 16 000 cm^{-1} as well as sharp and weak bands characteristic of f−f transitions in Er^{3+}. According to the literature,[1,2] the intense bands are assigned to transitions of the $[Pt(CN)_4]^{2-}$ chains. Our crystal was too thick to allow a direct measurement of the maximum of the lowest $[Pt(CN)_4]^{2-}$ band, assigned to $^1A_{1g}(5d_{z^2}, 6s) \rightarrow E_u(6p_z, \pi^*)$.[1,2,8] However, its position can be estimated to lie at about 17 000 cm^{-1} at 13 K. In the yellow form the $[Pt(CN)_4]^{2-}$ bands are shifted by about 4000 cm^{-1} to higher energy, whereas the f−f-transitions occur at the same energies.

Figure 4 shows the $\vec{E} \perp \vec{c}$ and $\vec{E} \parallel \vec{c}$ polarized emission spectra of $Er_2[Pt(CN)_4]_3 \cdot 21H_2O$ and $Er_2[Pt(CN)_4]_2 \cdot SO_4 \cdot 11.5H_2O$ at 13 K, respectively. They are strongly polarization-dependent, confirming the anisotropic character of the Pt−Pt interactions.

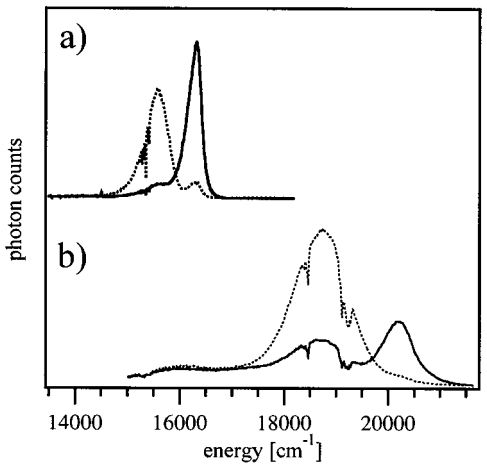

Figure 4. $\vec{E} \perp \vec{c}$ (···) and $\vec{E} \parallel \vec{c}$ (−) polarized emission spectra of $Er_2[Pt(CN)_4]_3 \cdot 21H_2O$ (red form) (a) and $Er_2[Pt(CN)_4]_2 \cdot SO_4 \cdot 11.5H_2O$ (yellow form) (b) at 13 K. Excitation wavelength is 457 nm.

The polarization is almost complete for the red form (Figure 4a), with the higher and lower energy bands polarized $\vec{E} \perp \vec{c}$ and $\vec{E} \parallel \vec{c}$, respectively. The energy difference between the two bands at 13 K is 3200 cm^{-1}, in good agreement with the onset of the strong polarized absorptions and the spectra reported by Yersin et al.[1,2] The same quality of polarized luminescence spectra could not be obtained for the yellow form (Figure 4b). This is due to a partial loss of water and a deterioration of the optical properties of this modification in the laser beam. The two band maxima can still be clearly identified, and their energy difference at 13 K is 3500 cm^{-1}. Superimposed on the broad luminescence bands we find sharp dips, which are due to radiative reabsorption of the Pt luminescence by the Er^{3+} ions. The luminescence of $Er_2[Pt(CN)_4]_3 \cdot 21H_2O$ is thus affected by the $^4I_{15/2} \rightarrow {}^4F_{9/2}$ absorption at 15 300 cm^{-1}, whereas the spectrum of $Er_2[Pt(CN)_4]_2 \cdot SO_4 \cdot 11.5H_2O$ shows the dips of the $^4S_{3/2}$ and $^2H_{11/2}$ excitations at 18 400 and 19 250 cm^{-1}, respectively.

The $[Pt(CN)_4]^{2-}$ absorption and emission bands are strongly temperature-dependent and are shifted to higher energy with increasing temperature. At room temperature the first $[Pt(CN)_4]^{2-}$ absorption bands occur with a maximum at about 19 000 and 22 200 cm^{-1} in the red and yellow structure, respectively. The $\vec{E} \parallel \vec{c}$ polarized absorption bands in the visible are more intense, and the band maxima in the spectra of our crystals cannot be determined. However, the relative positions of the first excitations in $\vec{E} \parallel \vec{c}$ and $\vec{E} \perp \vec{c}$ polarizations can be derived from the polarized luminescence spectra in Figure 4. The energies of the absorption and emission bands strongly correlate with the intracolumnar Pt−Pt distance R. A dependence of their energies with R^{-3} was found in a series of CP's. This behavior was rationalized by assuming dipole−dipole interactions between nearest neighbors within the $[Pt(CN)_4]^{2-}$ chains.[6] Corresponding transitions are thus shifted by $2e^2|M|^2/R^3$ to lower energy in the stack compared to the free $[Pt(CN)_4]^{2-}$ band, where M is the transition dipole moment in the $[Pt(CN)_4]^{2-}$ ion and R is the Pt−Pt distance within the columns. The relationship between corresponding absorption bands and the distance R is therefore given by the following equation:[7,8]

$$\tilde{\nu}_{abs} = a - bR^{-3} \qquad (1)$$

where a and b are characteristic of a specific transition. A similar relationship holds for the emission maxima. For the lowest energy $\vec{E} \perp \vec{c}$ polarized absorption of the CP's $a = 43.9 \times 10^3$ cm^{-1} and $b = 8.0 \times 10^5$ cm^{-1} Å^3 were found.[13]

Because we have determined the Pt−Pt distance of the title compounds, we are in a position to check the above correlation for the ErCP's. Both forms contain two different in-chain Pt−Pt distances, and in the most simple approximation we take the average of the two values to calculate the position of the absorption bands. For the red structure we find a mean Pt−Pt distance of 3.1758(8) Å, whereas the averaged Pt−Pt distance of the yellow form equals 3.3345(18) Å, resulting in calculated transition energies of 18 900 and 22 000 cm^{-1}, respectively. These values are in nice agreement with the experimentally determined room-temperature energies of 19 000 and 22 200 cm^{-1}, respectively. Thus, both modifications fit into the series of CP's.

Because the difference between the two Pt−Pt distances is larger in the yellow than in the red structure, we expect broader absorption and emission bands for the former compound, provided that nearest-neighbor interactions are responsible for the band shifts. That is exactly what is seen in the luminescence spectra of Figure 4.

Acknowledgment. We thank N. Furer for giving hints during the synthesis, V. Gold, U. Graf, A. Müller, Ch. Reinhard and M. Weiss for their help in solving the crystal structure and K. Krämer for his support in analyzing the structures of both modifications.

Supporting Information Available: One X-ray crystallographic file, in CIF format. This material is available free of charge via the Internet at http://pubs.acs.org.

IC991137X